

will occur, for an impurity radius such that the attractive and repulsive potentials are of comparable magnitude. Such a minimum apparently occurs in Ge for ions with a radius of approximately 1 Å, which corresponds rather closely to that of Cu (0.96 Å). The activation energy for the diffusion of Cu in Ge is 0.33 eV or less.¹ The diffusion activation energy for Li, which has a considerably smaller ionic radius (0.62 Å) is approximately 0.5 eV. The situation may be qualitatively similar in rutile with the minimum activation energy occurring at a somewhat smaller ionic radius. If the ionic radius of Li corresponds roughly to such a

minimum in rutile, any lattice strain would be likely to increase the diffusion activation energy. This also would account for failure to detect diffusion of Na⁺ (ionic radius 0.97 Å). Also, the difference in saddle-point configuration due to the anisotropy of rutile explains, at least qualitatively, the observed difference in diffusion rates parallel and perpendicular to the *C* axis.

The ease with which diffusion activation energy can be measured in this material and the extreme mathematical simplicity of the data analysis suggests that this system may be a very useful one for purposes of comparison with theory as it is developed.

Electrons in Bi-Sb Alloys

DALE M. BROWN AND S. J. SILVERMAN

General Electric Research Laboratory, Schenectady, New York

(Received 12 February 1964; revised manuscript received 2 June 1964)

Galvanomagnetic and thermoelectric measurements have been performed on doped and undoped Bi₈₅Sb₁₅-alloy single crystals. The thermal gap, obtained from the temperature variation of resistivity on high-purity *n*- and *p*-type samples, is 0.024 ± 0.003 eV, a significantly larger value than the previously measured maximum gap (0.014 eV) for this system. Hall data on Te-doped samples indicate that two Te atoms must be added to the crystal to add one additional free electron. Transport properties have been analyzed for Te-doped samples at 20 °K, using a multivalley conduction band. The magnitudes of the Seebeck and Hall coefficients indicate that most of the electrons must reside in three (not six) bismuth-like tilted ellipsoids. However, the lack of agreement between experiment and calculations based on the three-ellipsoid model for the ratio $\rho_{33, 11} : \rho_{33, 33}$ suggests the possible existence of a small number of electrons in an additional electron ellipsoid along the trigonal axis.

INTRODUCTION

THE thermoelectric and thermomagnetic properties of Bi-Sb alloys have recently received considerable attention.¹ However, little has been done in characterizing the basic band structure and transport properties of these alloys, nor have they been used extensively to understand the basic properties of bismuth.^{2,3} By performing transport measurements on doped and undoped Bi₈₅Sb₁₅ alloys, our purpose was to ascertain (1) the value of the thermal gap, (2) the number of Te atoms required to produce one additional free electron, (3) the valley multiplicity of the conduction band, and (4) the electron mobility tensor components. Conclusions based on resistivity, Hall and Seebeck coefficient data were checked against magneto-resistance data.

¹ G. E. Smith and R. Wolfe, *J. Appl. Phys.* **33**, 841 (1962); R. Wolfe and G. E. Smith, *Appl. Phys. Letters* **1**, 5 (1962); R. Wolfe, *Semicond. Prod.* **6**, 23 (1963); C. F. Gallo, B. S. Chandrasekhar, and P. H. Sutter, *J. Appl. Phys.* **34**, 144 (1963); S. R. Hawkins, J. H. Harshman, and G. M. Enslow, *Bull. Am. Phys. Soc.* **7**, 621 (1962).

² H. Jones, *Proc. Roy. Soc. (London)* **A147**, 396 (1934); D. Shoenberg and M. Z. Uddin, *ibid.* **A156**, 687 (1936); N. Thompson, *ibid.* **A155**, 111 (1936); **A164**, 24 (1937); V. Heine, *Proc. Phys. Soc. (London)* **A69**, 513 (1956).

³ A. L. Jain, *Phys. Rev.* **114**, 1518 (1959).

BACKGROUND—BISMUTH

The semimetallic properties of bismuth are caused by slightly overlapping electron-hole bands. The conventional model is represented by a single-hole band on the trigonal axis with a density of states effective mass of 0.16 m_0 , overlapping three- or six-electron ellipsoids located on the binary axes, but tilted slightly out of the basal plane. Many other more complicated models have been proposed because a vast and somewhat confusing amount of information has been published on the band structure and electrical properties of bismuth. However, there now appears to be relatively consistent agreement on the values for the effective masses of electrons on the Fermi surface. Further verification concerning the exact number of equivalent electron constant energy surfaces has been impeded by recent and often contradictory observations relating to the total electron concentration and the magnitude of the direct optical-band gap between the electron-band minimum and the valence band. The present situation is summarized in Table I where α_1 , α_2 , and α_3 are the eigenvalues of the reciprocal effective mass tensor; $\langle m \rangle / m_0 = (\alpha_1 \alpha_2 \alpha_3)^{-1/3}$ is the density of states effective mass for a parabolic band, E is the Fermi energy, E_0 is

TABLE I. Electrons in bismuth, $T=4^\circ\text{K}$.

Method or model	α_1	α_2	α_3	$\langle m \rangle / m_0$	$E(\text{eV})$	$E_0(\text{eV})$	$N/10^{17}$	$n/10^{17}$ (calculated)
de Haas-van Alphen ^a	417	0.396	40.8	0.053	0.018			
Cyclotron absorption ^b	167	0.99	101	0.039	0.018		2.5	
Cyclotron absorption ^c	114	0.56	47	0.070				
Infrared absorption ^d	133	0.59	91	0.052			4.4	
de Haas-van Alphen ^e	202	0.86	71	0.043	0.022	0.046	5.8	
Hall coefficient ^f							≤ 4.1	
Cyclotron and optical absorption ^g	119	0.57	103 ^h	0.052			3.9	
Galvanomagnetic ⁱ							2.5	
Cyclotron absorption ^j	162	0.765	87	0.045				
NENP ^j				0.045	(0.025) ^q	(0.015) ^q		0.8
Cyclotron absorption ^k	141	0.584	87.3	0.052				
NENP ^k				0.052	(0.022) ^q	(0.044) ^q		1.3
EP ^k				0.052	(0.022) ^q			1.8 ^p
Magneto-optical ^l					0.022	0.024		
Magneto-optical ^m					0.025	0.015		
Bi-Sb alloys ⁿ						0.007		
Infrared reflectivity ^o					0.027			

^a D. Shoenberg, Proc. Roy. Soc. (London) **A170**, 341 (1939); Phil. Trans. Roy. Soc. London **A245**, 1 (1952).

^b J. E. Aubrey and R. G. Chambers, Phys. Chem. Solids **3**, 128 (1957).

^c J. K. Galt, W. A. Yager, F. R. Merritt, B. B. Cetlin, and A. D. Brailsford, Phys. Rev. **114**, 1396 (1959).

^d See Ref. 14.

^e See Ref. 6.

^f See Ref. 8.

^g Based on a reinterpretation of data in Refs. c and d. See Ref. f.

^h The *eigenvalues* of the reciprocal electron effective-mass tensor published in Ref. f Eq. (4) ($\alpha_{1,2,3}=119, 2.05, 101$) are incorrect. The authors are in agreement with this correction.

ⁱ See Ref. 11.

^j See Ref. 7.

^k See Ref. 9.

^l W. E. Engeler, Phys. Rev. **129**, 1509 (1963).

^m R. N. Brown, J. G. Mavroides, and B. Lax, Phys. Rev. **129**, 2055 (1963); a previously published energy gap of $E_0=0.047$ eV [R. N. Brown, J. G. Mavroides, M. S. Dresselhaus and B. Lax, Phys. Rev. Letters **5**, 243 (1960)] is corrected here.

ⁿ See Ref. 3.

^o L. C. Hebel and P. A. Wolff, Phys. Rev. Letters **11**, 368 (1963).

^p The calculated $n=1.35 \times 10^{17}/\text{cc}$ in Ref. 9 [Eq. (31)] contains an error. The author agrees.

^q Values used in calculations but obtained from other publications.

the value of the optical gap, and N is the total electron concentration.

It has been shown that the electronic Fermi surface is not strictly ellipsoidal-parabolic (EP). A non-ellipsoidal, nonparabolic (NENP) model of the conduction-band ellipsoids for which the tensor mass components depend on the energy, proposed by Cohen⁴ and Lax⁵, has been used by Weiner,⁶ Smith,⁷ Jain and Koenig,⁸ and Kao⁹ in various analytical forms to calculate carrier population per ellipsoid.

The problems of interpretation using this NENP model are twofold. First of all, this model has never been successfully tested. Many workers have interpreted their experimental results assuming that the model is correct *a priori*. The second problem is the determination of the direct gap between the valence band and the conduction-band minimum which governs the amount of nonparabolicity in the electron valleys and, subsequently, the total population of carriers in

each valley. Depending on the values chosen for E , E_0 , and $\langle m \rangle$ (Table I), the calculated carrier concentration per ellipsoid n can easily vary by a factor of 2, as seen in a summary of Kao's⁹ and Smith's⁷ results in Table I. The largest n , which naturally comes from an EP model calculation, is also included. One can obtain a valley multiplicity ranging from 2 to 7 using these numbers for n and the various N 's in Table I.

The experimental values for N are fairly scattered. For instance, Weiner's value of $N=5.8 \times 10^{17}/\text{cc}$ seems unusually high. This value of N was obtained by de Haas-van Alphen measurements on a series of Te-doped bismuth samples with the assumption that each added Te atom adds one electron and that there are, therefore, six complete ellipsoids. This assumption has already been questioned by Jain and Koenig.⁸ Our experiments with Bi-Sb alloys show that it takes two Te atoms to produce one added electron and that most, if not all, of the electrons must reside in three bismuth-like tilted ellipsoids.

EXPERIMENTAL TECHNIQUES

The methods used to grow the Bi-Sb alloy crystals have been described by Brown and Heumann.¹⁰ Precautions were taken to reduce the amount of constitutional supercooling and resultant macro- and micro-

¹⁰ D. M. Brown and F. K. Heumann, J. Appl. Phys. **35**, 1947 (1964).

⁴ M. H. Cohen, Phys. Rev. **121**, 387 (1961).

⁵ B. Lax, Bull. Am. Phys. Soc. **5**, 167 (1960); B. Lax, J. G. Mavroides, H. J. Zeiger, and R. J. Keyes, Phys. Rev. Letters **5**, 241 (1960); B. Lax and J. G. Mavroides, *Advances in Solid State Physics* (Academic Press Inc., New York, 1960), Vol. 11; B. Lax, *The Fermi Surface* (John Wiley & Sons, Inc., New York, 1960).

⁶ D. Weiner, Phys. Rev. **125**, 1226 (1962).

⁷ G. E. Smith, L. C. Hebel and S. J. Buchsbaum, Phys. Rev. **129**, 154 (1963); G. E. Smith, Phys. Rev. Letters **9**, 487 (1962).

⁸ A. L. Jain and S. H. Koenig, Phys. Rev. **127**, 442 (1962).

⁹ Yi-Han Kao, Phys. Rev. **129**, 1122 (1963).

inhomogeneity that can normally occur while growing these alloy crystals.

The growth conditions (temperature gradient at the growing interface of about 60°C/cm and a growth rate of between 0.4 and 1.6 mm/h) for the crystals used here represent a considerable improvement in the Bi-Sb compositional uniformity compared to crystals grown at much faster speeds (e.g., ≥ 5 mm/h). The degree of macrohomogeneity in these samples, as characterized by variations in Sb content averaged over millimeter distances, is $15 \pm 1\%$ Sb. The degree of microhomogeneity is at worst $15 \pm 3\%$ Sb through distances of 0.1 mm as determined by electron beam microprobing.

Single-crystal sections of the alloy ingots were oriented by locating the basal plane perpendicular to the c or trigonal $\langle 3 \rangle$ axis by cleavage; and back-reflection x-ray Laue photographs of this cleavage surface were used to locate the binary $\langle 1 \rangle$ and bisectrix $\langle 2 \rangle$ axes. All sample cutting was done by using an electrical discharge machine which reduces the possibility of straining the samples. Measurements were made on oriented bars of typical dimensions $10 \times 2 \times 1.5$ mm³.

Hall measurements on bars cut with the longitudinal axis perpendicular to $\langle 3 \rangle$ afforded simultaneous measurements of the two independent Hall coefficients R_s and R_p , where R_s is obtained by measuring the Hall effect when H is perpendicular to $\langle 3 \rangle$, but parallel to $\langle 1 \rangle$ or $\langle 2 \rangle$, and R_p is obtained by measuring Hall voltages when H is parallel to $\langle 3 \rangle$. The sign of these two Hall coefficients is determined by the sign of the potential developed in the $\mathbf{I} \times \mathbf{H}$ direction, which is according to convention. Measurements of R_s on pairs of samples with their lengths parallel or perpendicular to $\langle 3 \rangle$ was a good method of determining their electrical compatibility, as it is *very* unsafe to arbitrarily assume any degree of homogeneity in these alloys.

Additional studies were performed to ensure electrical homogeneity. These included (1) sets of measurements at 20°K on many samples of the same type to test for electrical homogeneity and (2) Hall coefficient profiles at 20°K using wire pressure probes. Wood's metal solder was used for attaching thermocouples and electrical leads. Precautions were taken to ensure that the solder spot was small enough and far enough from the ends of the samples to eliminate effects due to shorting the Hall voltage.

Most of the measurements were made at temperatures of 20°K or higher. This has three important advantages over measurements made at 4°K. (1) The low-field region in which the Hall voltage is proportional to H and the magnetoresistance is proportional to H^2 is extended to higher fields because the mobilities are lower. This situation makes the measurements easier because it increases the size of the signal and makes the measurements of magnetic field easier (with bismuth at 4°K, millimicrovolt sensitivities, and fields

of about 1 G are required for the low-field region).¹¹ (2) The mean free paths are considerably reduced at 20°K which helps eliminate effects due to sample size limitations. In order to eliminate size effects, the smallest dimension of our samples was at least 100 times the mean free path at 20°K. Calculations by Ham and Mattis¹² show that this is more than adequate. At 4°K much more massive samples would be required.^{11,13} (3) Higher temperatures also help to reduce the importance of impurity scattering. The absence of impurity scattering is important to the correctness of the analysis and theoretical model. It should be pointed out that the large dielectric constant in these materials (~ 100)¹⁴ also helps considerably to reduce ionized impurity scattering. In addition, 20°K is a sufficiently low temperature to make our n -type Bi₈₅Sb₁₅ samples extrinsic semiconductors.

A number of different measurements were made on our Bi-Sb alloys. These included measurements as a function of temperature of the two low-field Hall coefficients, the two independent Seebeck coefficients (S_{11} and S_{33}), and the two resistivity tensor components (ρ_{11} and ρ_{33}). The two Hall coefficients were also measured at 20°K as a function of magnetic field and five of the eight independent components¹⁵ of the second power magnetoresistance tensor were measured in the low-field region at 20°K.

Measurements were made in a vacuum cryostat and by dip-stick techniques in liquid H₂. Most of the temperature measurements were made with standard Cu-constantan thermocouples, though for $T < 60$ °K, carefully calibrated Cu versus Au-2.1% Co thermocouples were substituted, there being the advantage of greater sensitivity in this low-temperature range.

All measurements were made using conventional dc techniques. Voltages were measured by type K-3 Leeds and Northrup potentiometer. Magnet calibration was done by using rotating-coil Rawson Type 824 and 720 fluxmeters which had been previously calibrated using proton resonance. Careful field-reversing procedures were used in order to eliminate hysteresis effects. For fields below 100 G, the field was continuously monitored.

EXPERIMENTAL RESULTS

All the measurements presented here were done on Bi₈₅Sb₁₅ alloys. Thermal gap measurements indicate that the gap at this concentration is sufficiently large to make one type of carrier transport, electrons or holes, predominate at 20°K. Such a situation lends itself well to a simpler type of band-structure analysis than that which must be used when both types of carriers are present.

¹¹ R. N. Zitter, Phys. Rev. **127**, 1471 (1962).

¹² F. S. Ham and D. C. Mattis, IBM J. Res. and Develop. **4**, 143 (1960).

¹³ A. N. Friedman and S. H. Koenig, IBM J. Res. and Develop. **4**, 158 (1960).

¹⁴ W. S. Boyle and A. D. Brailsford, Phys. Rev. **120**, 1943 (1960).

¹⁵ H. J. Juretschke, Acta Cryst. **8**, 716 (1955).

Figures 1, 2, and 3, which are respective plots of resistivity, Hall coefficients, and Seebeck coefficients versus $1/T$, exhibit the general semiconducting, albeit very narrow band gap, nature of this alloy. At 300°K all these alloys, doped and undoped, have negative Seebeck coefficients and negative Hall coefficients.

The features of the curves in Figs. 1-3 can be understood qualitatively as follows. Because of the small thermal gap and because the relative ratio of hole to electron masses is greater than one, the Fermi energy at 300°K is very close to the electronic band edge. All these samples are n type at 300°K because the average electron mobilities are higher than those of holes. As the temperature is lowered, each sample becomes extrinsically n or p type depending on the ratio of donor-to-acceptor impurities. It must be pointed out that relatively low concentrations of impurities may produce impurity banding in these systems because of the large dielectric constant and small effective masses. A hydrogenic model indicates impurity activation energies of only 7×10^{-5} eV.

Investigations for traces of Pb, Sn, and Te indicate that in the undoped alloys the impurity concentrations would be about 5 ppm for Pb and less than 2 ppm for

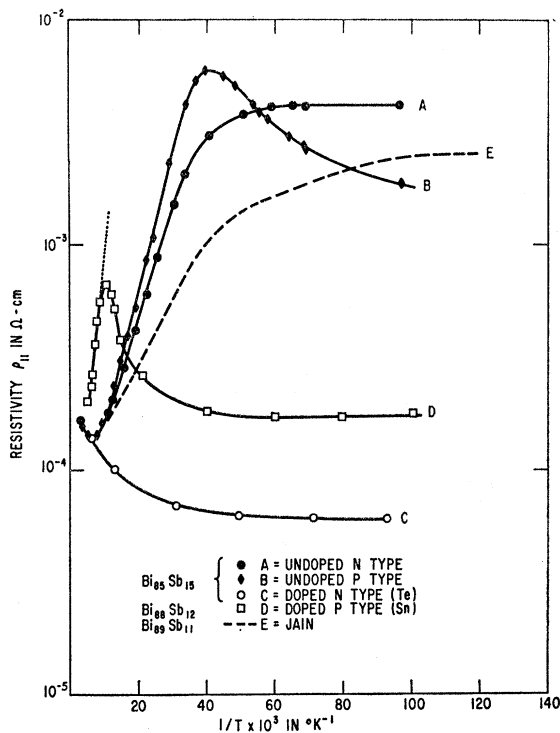


FIG. 1. Resistivity ρ_{11} versus $1/T$. Samples A, B, C are $\text{Bi}_{85}\text{Sb}_{15}$ alloys which are undoped n - and p -type crystals and an n -type crystal intentionally doped with Te, respectively. Crystal D is a $\text{Bi}_{88}\text{Sb}_{12}$ crystal purposely doped with Sn to make it p -type. Sample E, dashed curve, is the curve used by Jain³ to ascertain a maximum thermal gap of 0.014 eV for the Bi-Sb solid solution system.

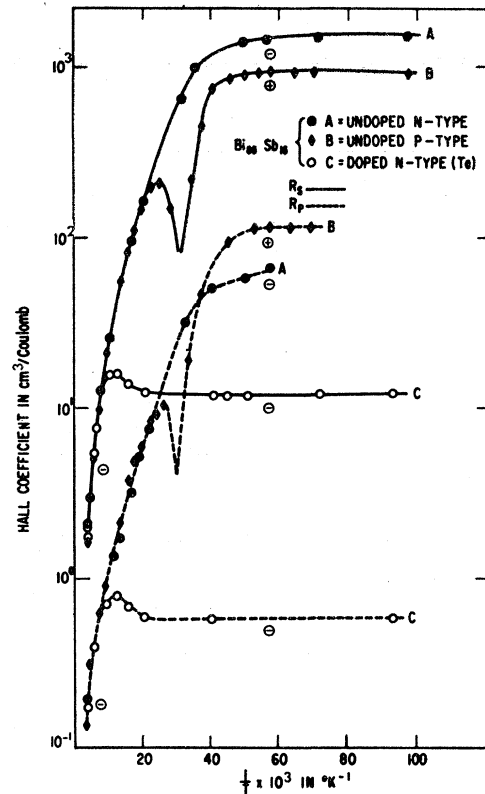


FIG. 2. Hall coefficients R_s and R_p versus $1/T$ for samples A, B, and C which are $\text{Bi}_{85}\text{Sb}_{15}$ alloys; undoped n - and p -type crystals A and B, respectively; and intentionally Te-doped, n -type sample C.

Sn and Te.¹⁶ The magnitude of R_s for the undoped samples is not inconsistent with these residual impurity concentrations. Samples A and B are pure, unintentionally doped n - and p -type samples. For the undoped n - and p -type samples, the magnitude of the Seebeck coefficients at low temperatures is greater than 200 $\mu\text{V}/^\circ\text{C}$ (Fig. 3). The large magnitude of these positive and negative Seebeck coefficients, indicative of Fermi energies below band edges, is convincing evidence that these alloys are real semiconductors (see Appendix). Samples C and D are, respectively, doped n -type (Te doped, about 20 ppm) and p -type (Sn doped, about 100 ppm) crystals. A summary of some of the electrical characteristics of these 4 samples is given in Table II. Figure 1 includes Jain's data (curve E) for an 11% Sb alloy from which he deduced a maximum thermal gap, E_t , of 0.014 eV for this system.³

As shown in the figures, at temperatures below 80°K, the values of the resistivity, Seebeck coefficient, and the Hall coefficient are very sensitive to the nature and the amount of impurities. There is also a consistency in both the temperature dependence and sign of all of these coefficients associated with any particular sample.

¹⁶ Chemical analyses performed by Ledoux and Company, Teaneck, New Jersey.

TABLE II. Galvanomagnetic and thermoelectric parameters in $\text{Bi}_{85}\text{Sb}_{15}$ alloys at $T = 20.4^\circ\text{K}$.

Sample	Longitudinal orientation	Resistivity ($\Omega\text{-cm}$)		Hall constant (cm^2/C)		Thermoelectric power ($\mu\text{V}/^\circ\text{C}$)	
		ρ_{11}	ρ_{33}	R_s	R_p	S_{11}	S_{33}
A Undoped n	(2)	3.4×10^{-3}	2.5×10^{-3}	-1300	-56	-262 ^a	
	(3)			-1300			
B Undoped p	(2)	5.0×10^{-3}		+1140	+100	+250	
C Te-doped n	(1)	6.5×10^{-5}	4.5×10^{-6}	-12	-0.58	-22.5	
	(3)			-13.5			
D Sn-doped p	(1)	1.65×10^{-4}		+25.5	+1.2	+16	
$\text{Bi}_{88}\text{Sb}_{12}$	(3)		1.65×10^{-4}	+33		+18	

^a At 25°K .

These observations are not in agreement with the sign of the Hall coefficients as measured by Jain³ on samples of this composition.¹⁷ According to Jain, R_s is positive for

all temperatures when the composition is greater than 3% Sb; whereas, R_p is always positive above 25°K , but positive or negative below 25°K according to whether the composition is, respectively, less than or greater than 11.5% Sb.

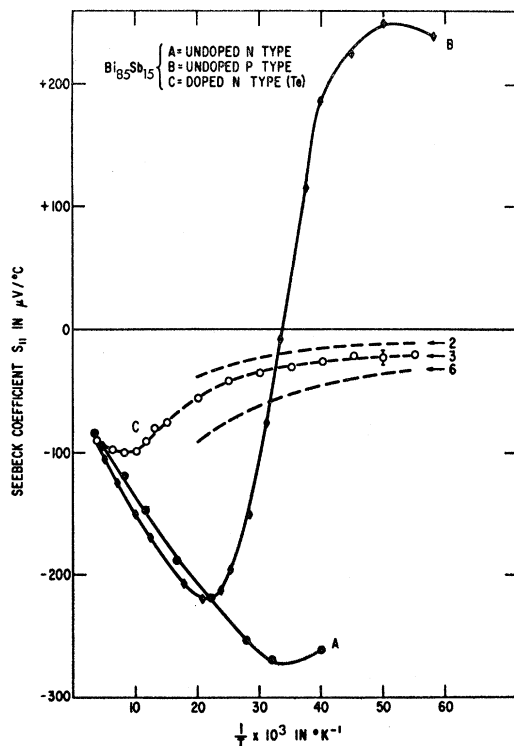


FIG. 3. Seebeck coefficient S_{11} versus $1/T$ for samples A, B, and C which are $\text{Bi}_{85}\text{Sb}_{15}$ alloys; undoped n - and p -type crystals A and B, respectively; and intentionally Te-doped n -type sample C.

¹⁷ Our results are in agreement with the R_s measurements on undoped 5 and 12% Sb alloys made by Kooi and Cuff *et al.* [J. H. Harshman, S. R. Hawkins, R. B. Lorst and J. L. Weaver, Lockheed Missiles and Space Company, Interim Engineering Report No. 3, March 1962 (unpublished)] who find R_s to be negative for $T > 77^\circ\text{K}$. See also G. A. Ivanov and A. M. Popov, *Fiz. Tverd. Tela* 5, 1754 (1963) [English transl.: *Soviet Phys.—Solid State* 5, 2409 (1964)].

THERMAL ENERGY GAP, E_t

Figure 1 shows a continuous increase in slope, proceeding from the undoped n -type specimen through the undoped p -type sample to the doped p -type sample. The situation is reminiscent of that which occurs in InSb where the electron to hole-mobility ratio is large and the conductivity in the exponential high temperature regions results from varying contributions of impurity and intrinsic conductivity.¹⁸

To a first approximation, the slope of $\ln(\text{resistivity})$ versus $1/T$ plots for undoped samples will be less than or greater than $E_t/2k$, depending on whether the sample is n type (curve A) or p type (curve B). In heavily doped p -type material (curve D), when the number of ionized acceptors approaches the intrinsic carrier concentration, the slope approaches a limiting value of E_t/k . The thermal gap will therefore lie somewhere between that given by setting the slope of the $\ln\rho$ versus $1/T$ plots for the undoped samples equal to $E_t/2k$.¹⁹ On this basis, the undoped n - and p -type samples give E_t 's of 0.021 and 0.027 eV, respectively. We therefore estimate that the gap for a $\text{Bi}_{85}\text{Sb}_{15}$ alloy is 0.024 ± 0.003 eV on the basis of these two n - and p -type undoped crystals. [The doped p -type crystal

¹⁸ N. B. Hannay, *Semiconductors* (Reinhold Publishing Corporation, New York, 1959), p. 392.

¹⁹ This assumes, of course, that the density of available states, and the mobilities of the carriers vary as T^{+P} and T^{-P} , respectively. It also assumes the correctness of an exponential law rather than using Fermi functions. The first assumption seems reasonable for undoped samples when the temperature is between 80 and 25°K (exponential region, Fig. 1), where density of available states and mobilities would be expected to vary like $T^{3/2}$ and $T^{-3/2}$, respectively. Using an exponential law rather than Fermi functions will give slightly larger values for E_t , but even if E_t is as small as $1 kT$, the error is only about 12%.

(Bi₈₈Sb₁₂), over the limited temperature range shown, yields $E_t=0.029$ eV on the basis of an E_t/k slope as shown by the dotted curve in Fig. 1.] The increase in measured gap over Jain's data may be due to (1) increased Bi-Sb homogeneity and/or (2) smaller amounts of electrically active residual impurities.

Te DOPING

Six quantitative chemical analysis¹⁶ of material adjacent to and on either side of the slices from which the electrical samples were taken from the Te-doped ingot indicate an average Te concentration of $1.01 \pm 0.13 \times 10^{18}$ Te atoms/cc. The Hall coefficients of a number of these Te-doped samples were carefully studied. The field variation of the two Hall coefficients is shown in Fig. 4. The Hall data were found to be essentially identical for these samples and Fig. 4 can be taken to represent a composite of the data. The error marks represent the variation obtained in R_s at 17 000 G for a number of measurements along the length of one sample obtained by moving small wire point probes.

The interpretation of the Hall data is as follows. The doping is sufficiently heavy in this sample to make the number of holes P essentially zero. At low fields the large difference between R_p and R_s is due, of course, to the lack of crystal symmetry and the nature of the mobility tensor. However, at very high fields both Hall coefficients should be equal to $(Ne)^{-1}$, where N is the total electron concentration.²⁰ This condition is being approached in Fig. 4 even though fields sufficiently high to make R_p exactly identical to R_s were not available. Such behavior and the essential constancy of R_s with field indicates that $R_s(200 \text{ G}) \leq 1/Ne \cong R_s(20\,000 \text{ G})$. The total electron concentration is then equal to $N = (4.8 \pm 0.6) \times 10^{17}/\text{cc}$, where the error includes the field variation of R_s , sample to sample variations, and any possible inhomogeneity in Te concentration. This result, together with the results of the six quantitative analyses for Te, gives a ratio of Te atoms/cc to electrons/cc of 2.1 ± 0.3 . This means that two Te atoms must be added to the Bi-Sb lattice in order to produce one additional free electron.

CONDUCTION BAND

Assuming for the moment that the usual ellipsoidal-parabolic model (EP) applies to the present situation, the number of equivalent electron valleys can be obtained unambiguously from our data in the following manner.

For the EP model, the carrier concentration N for a multivalley system with a degenerate Fermi carrier population is

$$N = Bn = B(2^{3/2}\pi/3h^3)m_0^{3/2}(\alpha_1\alpha_2\alpha_3)^{-1/2}E^{3/2}, \quad (1)$$

where n is the carrier concentration per valley, B is the

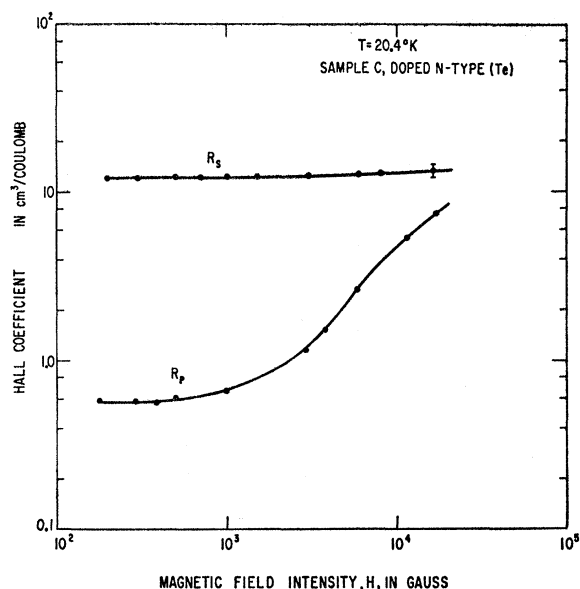


FIG. 4. The two independent Hall coefficients R_s and R_p of the Te-doped Bi₈₈Sb₁₂ alloy, sample C, versus H .

number of equivalent valleys, $\alpha_1\alpha_2\alpha_3$ are the eigenvalues of the effective mass tensor, and E is the Fermi energy. Using an $\alpha_1\alpha_2\alpha_3$ product of $7247 m_0^3$, which is an average of the three most recent sets of effective-mass data for bismuth and which also represents the most often occurring density of states effective mass ($0.052 m_0$) in Table I, one can calculate E for various valley multiplicities. B 's of 2, 3, 6 give Fermi energies of 0.027, 0.021, and 0.013 eV, respectively. The proper choice of E or B can be obtained by using the Seebeck coefficient data.

The Seebeck coefficient for a single-type carrier model and acoustic-mode lattice scattering is given by²¹

$$S_{11} = S_{33} = S = 86.2 \{ [2F_1(\epsilon)/F_0(\epsilon)] - \epsilon \} \mu\text{V}/^\circ\text{C}, \quad (2)$$

where F_1 and F_0 are the usual Fermi-Dirac integrals of order 1 and 0, respectively, and $\epsilon = E/kT$. Notice that in this case the Seebeck coefficient is isotropic. This would not be so if other carriers were present at another band edge. For instance, the presence of holes in bismuth makes $S_{33} \cong 2S_{11}$.²² Samples cut along the $\langle 3 \rangle$ direction are very susceptible to stress, and crack easily. Because of this difficulty, we were not able to determine whether or not S_{33} was exactly identical to S_{11} . However, we were able to ascertain that $S_{33} = S_{11} \pm 20\%$ below 50°K . The calculations of S versus $1/T$ using Eq. (2) and Fermi energies of $E=0.03$, 0.021, and 0.013 eV are compared in Fig. 3. (It must be recalled that the Hall coefficients and, therefore, N and E for this sample are constant below 50°K .) The

²¹ R. W. Ure, Jr., *Thermoelectricity—Science and Engineering*, edited by R. R. Hickey and R. W. Ure, Jr. (Interscience Publishers, Inc., New York, 1961).

²² B. S. Chandrasekhar, *Phys. Chem. Solids* **11**, 268 (1959).

²⁰ J. A. Swanson, *Phys. Rev.* **99**, 1799 (1955).

curve for $E=0.021$ eV fits the experimental data almost exactly. The error marks at 20°K indicates the spread in calculating the Seebeck coefficient at 20°K with a range of Fermi energies between 0.019 and 0.023 eV, which represents a calculated Seebeck coefficient of $23 \mu\text{V} \pm 12\%$. E is therefore determined to be 0.021 ± 0.002 eV, which indicates a probable valley multiplicity, B , of 3.

Having determined E , we can now justify the assumption that $P \ll N$ at 20°K. Since the thermal gap, as determined by the undoped alloys is (0.024 ± 0.003) eV, the number of holes is then

$$P = 2\pi^{-1/2} N_v F_{1/2}(-\epsilon_t - \epsilon) \cong N_v \exp(-\epsilon_t - \epsilon),$$

where

$$N_v = 2(2\pi m_i kT/h^2)^{3/2} \quad \text{and} \quad \epsilon_t = E_t/kT. \quad (3)$$

Equation (3) makes $P \ll N$ for reasonable hole effective masses between $0.1m_0$ and $2m_0$. In fact, the density-of-states effective mass and/or multiplicity of hole bands would have to be impossibly high to make $P=N$. $P \ll N$ is also a good assumption for sample A.

The previously given determination of ellipsoidal multiplicity is, of course, dependent on the accuracy of the EP model which assumes that the valleys are parabolic with a density-of-states effective mass independent of energy. An estimate of the degree of nonparabolicity in these bands, insofar as it affects the density of states effective mass, can be made by examining the carrier concentration in the undoped n -type sample (sample A), where the Fermi energy is approximately $1kT$ below the band edge at 25°K ($E \cong -0.002$ eV) as determined from the value of the Seebeck coefficient [Eq. (2)]. Using the 3 EP model and the carrier concentration as determined by Hall coefficient versus magnetic field (similar in nature to that shown in Fig. 4), an $\langle m \rangle$ of $0.044m_0$ was calculated. This density-of-states effective mass should be characteristic of the bottom of the valley. It is only slightly smaller than the $0.052m_0$ used above.²³ An EP calculation using respectively $\langle m \rangle = 0.044m_0$ and $0.052m_0$ together with the *minimum* and *maximum* E , as estimated from the Seebeck coefficient of Sample C (Te-doped sample), gives

$$1.1 \leq n/10^{17} \leq 1.9.$$

Since the Hall coefficient measurements (Fig. 4) give

$$N = (4.8 \pm 0.6) \times 10^{17}/\text{cc},$$

the ellipsoidal multiplicity B is therefore

$$2 < B < 5.$$

²³ It must be emphasized that the valley nonparabolicity in Bi and in Bi-Sb alloys containing less than 15% Sb, where band edges are much closer together, may be much greater. For instance, Smith's⁷ cyclotron resonance experiments in a $\text{Bi}_{99}\text{Sb}_1$ alloy give effective mass components about a factor of two smaller than those for Bi; Kao *et al.*'s [Yi-Han Kao, R. L. Hartman, and R. D. Brown, III, *Bull. Am. Phys. Soc.* **9**, 96 (1964)] experiments in $\text{Bi}_{99}\text{Sb}_1$ alloys also indicate strong deviations from nonparabolicity.

Since only ellipsoidal multiplicities of 1, 2, 3, 6, and 12 are allowable by crystal symmetry,²⁴ we can conclude that the number of equivalent Bi-type electron valleys *must* be three.

It could be argued that the analysis used above, which is essentially based on density-of-states arguments, might fail to detect other groups of electrons and that the agreement between the Fermi energies obtained from the Seebeck coefficient and the Hall coefficient data is somewhat coincidental. Because of this, we must ascertain how well the three-ellipsoid-multivalley model fits the magnetoresistance data.

The proposed conduction-band model consists of the usual set of ellipsoids each of which is centered on a binary axis and tilted slightly out of the basal plane. For such a model, the electron mobility tensor in the crystal axes coordinate system is

$$\mu = \begin{pmatrix} \mu_1 & 0 & 0 \\ 0 & \mu_2 & \mu_4 \\ 0 & \mu_4 & \mu_3 \end{pmatrix}. \quad (4)$$

The ellipsoidal tilt angle θ is given by $2\mu_4/(\mu_2 - \mu_3) = \tan 2\theta$ and is measured between the "3" axis of the tilted ellipsoid and the trigonal $\langle 3 \rangle$ axis of the crystal.

Assuming the existence of intravalley scattering, degenerate Fermi statistics, and isotropic or weakly anisotropic relaxation times within each ellipsoid,¹¹ one can analyze the two independent components of the resistivity and low-field Hall coefficient tensor. These terms are obtained from conductivity tensor equations derived independently by Freedman,²⁵ Epstein and Juretschke,²⁶ and Zitter,¹¹ who have previously considered the galvanomagnetic effects of Sb and Bi, respectively. In the case of the three-ellipsoid model, we have

$$\begin{aligned} \rho_{11} &= (2/eN)(\mu_1 + \mu_2)^{-1}, \\ \rho_{33} &= (1/eN)(\mu_3)^{-1}, \\ -R_p &= (4/eN)[\mu_1\mu_2/(\mu_1 + \mu_2)^2], \\ -R_s &= (1/eN)\{1 - [\mu_4^2/(\mu_1 + \mu_2)\mu_3]\}. \end{aligned} \quad (5)$$

The behavior of the Hall coefficient curves in Fig. 4 are easily understood if the shape of the bands are similar to those in bismuth where $m_2 > m_1, m_3$ and $\mu_1, \mu_3 \gg \mu_2, \mu_4$ so that

$$R_s(0) \cong 1/Ne \gg R_p(0) \quad \text{with} \quad R_p \rightarrow R_s \rightarrow 1/Ne$$

in the high-field limit.

The mobility tensor components μ_1, μ_2 , and μ_3 are directly obtainable using Eq. (5) and the total electron concentration $N = 4.8 \times 10^{17}/\text{cc}$ as determined from R_s in Fig. 4. These are shown in Table III. Table III also includes the results of similar, but somewhat approxi-

²⁴ J. R. Drabble and R. Wolfe, *Proc. Phys. Soc. (London)* **B69**, 1101 (1956).

²⁵ S. J. Freedman and H. J. Juretschke, *Phys. Rev.* **124**, 1379 (1961).

²⁶ S. Epstein and H. J. Juretschke, *Phys. Rev.* **129**, 1148 (1963).

TABLE III. Transport parameters for *n*-type Bi₈₅Sb₁₅ alloys at 20°K (three-ellipsoid model).

Sample	N/cc	μ_1 (cm ² /V-sec)	μ_2 (cm ² /V-sec)	μ_3 (cm ² /V-sec)	E (eV)
C (Te doped)	$(4.8 \pm 0.6) \times 10^{17}$	4.0×10^6	0.045×10^6	2.9×10^6	+0.021
A (undoped)	4.7×10^{15}	7.7×10^6	0.08×10^6	5.4×10^6	-0.002

mate calculations for the undoped *n*-type sample A which is not degenerate at 20°K.

MAGNETORESISTANCE

The low-field magnetoresistance data for the Te-doped 15% Sb alloy are shown in Fig. 5.

In Fig. 5 the magnetoresistance factors $\Delta\rho/\rho_0$ are proportional to H^2 below a few hundred gauss. The values of the second power magnetoresistance tensors $\rho_{11,11}$, $\rho_{11,22}$, $\rho_{11,33}$, $\rho_{33,11}$, and $\rho_{33,33}$ are given in Table IV where they are compared to those values computed for a tilted three-ellipsoid conduction band. (The same pattern of $\rho_{11,22} \cong \rho_{11,11} > \rho_{33,11} > \rho_{33,11}$ and $\rho_{33,11} \cong 5 \rho_{33,33}$ is repeated in the undoped *n*-type sample A. However, since the Fermi level is below the band edge, these data cannot be subjected to an exact analysis.) To a first approximation, assuming $\mu_1 > \mu_4$, μ_2 on the basis of bismuth-like bands, these parameters are approximately as follows:

$$\begin{aligned}
 \rho_{11,11} &\cong \rho_{11,22} \cong (1/2eN)\mu_3, \\
 \rho_{11,33} &\cong (2/eN)\mu_2, \\
 \rho_{33,11} &\cong (1/2eN)(\mu_4^2/\mu_3), \\
 \rho_{33,33} &= (1/eN)\mu_1(\mu_4/\mu_3)^2 \cong 2(\mu_1/\mu_3)\rho_{33,11}.
 \end{aligned}
 \tag{6}$$

As indicated by Eq. (6), $\rho_{33,11}$ and $\rho_{33,33}$ are basically

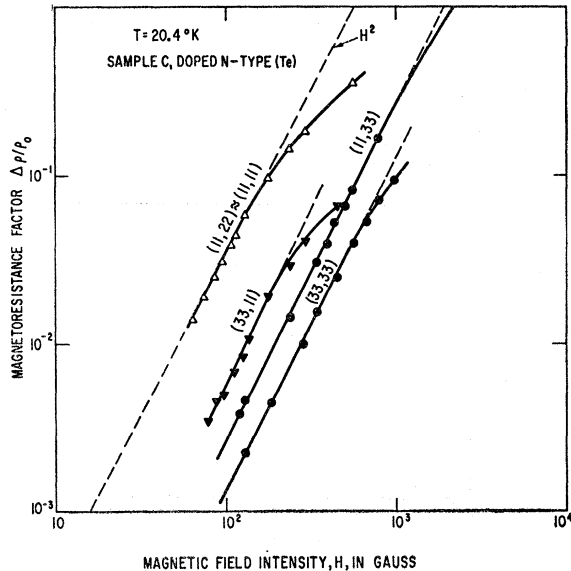


FIG. 5. Magnetoresistance factors, $\Delta\rho/\rho_0$ versus H as measured on the Te-doped Bi₈₅Sb₁₅ alloy from which the second-power magnetoresistance tensors $\rho_{11,22}$, $\rho_{33,11}$, $\rho_{11,33}$, $\rho_{33,33}$ can be obtained.

tilt angle terms in the tilted ellipsoidal model and disagreement between the calculated²⁷ and experimental values indicates that this type of a conduction-band model cannot account for all the magnetoresistance tensor components (see Table IV).

An alternative model has been tested. This is suggested by the fact that in bismuth, $\rho_{33,11} \cong \rho_{11,22} > \rho_{33,33}$.¹¹ The major contribution to $\rho_{33,11}$ in bismuth is due to the holes that are located in an ellipsoid on the trigonal axis. In bismuth, $\rho_{33,33}$ remains an electron ellipsoidal tilt angle term. This type of a comparison with the magnetoresistance tensors of bismuth suggests that the larger than expected magnetoresistance tensor component $\rho_{33,11}$ could be caused by a small number of electrons in an ellipsoid on the trigonal axis. The calculated tensor components using this 3-1 model are much closer to all the experimentally observed values than for the three-ellipsoid model. A computer technique was used to explore some of the possible solutions for this model with the limitation that $\mu_2 \geq 1000$ cm²/V-sec, which is a reasonable value for the elimination of the Hall effect anisotropy above 40 000 G. The results of this exploration are shown in Table IV. In Table IV

TABLE IV. Galvanomagnetic data Te-doped Bi₈₅Sb₁₅ ($T=20^\circ\text{K}$). Resistivities in $\Omega\text{-cm} \times 10^6$. Hall coefficients in cc/coulomb; mobilities in cm²/(V-sec) $\times 10^{-6}$; magnetoresistance in cm⁶/(V-sec-coulomb) $\times 10^{-6}$.

Parameter	Experimental ^a	3E Model	3-1 Model	
N	4.8×10^{17}			
ρ_{11}	6.5			
ρ_{33}	4.5			
$-R_p$	0.58			
$\rho_{33,33}$	0.06 ± 0.01			
N_2/N_1		0	0.02	0.15 ± 0.05
ν_1		...	3 ± 1	0.5 ± 0.3
ν_3		...	9 ± 1	5 ± 4
$-R_s$	12 ± 1	13	13	13 ± 2
μ_1		4.0	4.0	4.5 ± 0.4
μ_2		0.044	0.02 ± 0.005	0.03 ± 0.01
μ_3		2.9	2.8	3 ± 1
μ_4		0.22	0.22	0.23
$\rho_{11,11}$	2.3	1.8	1.8	2.0 ± 0.4
$\rho_{11,22}$	2.4 ± 0.3	1.8	1.8	2.0 ± 0.4
$\rho_{11,33}$	0.18	0.11	0.14 ± 0.03	0.10 ± 0.03
$\rho_{33,11}$	0.30	0.01	0.27 ± 0.02	0.2 ± 0.1

^a The error figures indicate the spread in measured values for six different samples

²⁷ The exact equations for the magnetoresistance tensor components in a crystallographic coordinate system can be obtained from Zitter's conductivity tensor equations.¹¹ (Zitter's exact expressions for $\rho_{11,22}$ and $\rho_{33,11}$ contain typographical errors. Zitter agrees.)

N_2 is the electron concentration in the ellipsoid on the trigonal axis with mobility components of ν_1 and ν_3 and N_1 is the concentration of the electrons in the three bismuth-like tilted ellipsoids. Two regions of improved fit were found, one region was found for a very small N_2/N_1 ratio of 0.02 and the other near a ratio of 0.15. The tolerance numbers include all calculations of closest fit. This model may suggest a means of resolving the discrepancy in the comparative magnitudes of $\rho_{33,11}$ and $\rho_{33,33}$ which occurs when comparing the data with the simple three-ellipsoid model, but does not prove that such a band exists. A 15% reduction in the number of electrons in the bismuth-like ellipsoids would not alter our conclusion that three of these ellipsoids, and not six,³ exist in the conduction band.

SUMMARY AND DISCUSSION

A set of transport measurements has been performed on a series of $\text{Bi}_{15}\text{Sb}_{15}$ alloys. These measurements indicate that (1) the intrinsic thermal gap of relatively pure undoped 15% Sb alloys is 0.024 ± 0.003 eV; (2) two Te atoms must be added to the crystal to produce one additional electron; (3) most, if not all, of the electrons must reside in three tilted bismuth-like electron ellipsoids; (4) the three tilted electron ellipsoids do not adequately describe all of the magnetoresistance results. This suggests a need to invoke the possible existence of a small number of electrons in an ellipsoid on the trigonal axis. However, we would emphasize that this model does not necessarily prove the existence of this additional electron ellipsoid, since the uniqueness of such a model cannot be proved from this set of measurements alone.

ACKNOWLEDGMENTS

We are indebted to Dr. W. E. Engeler, Dr. F. S. Ham, and Dr. R. O. Carlson for their constructive contributions to the discussions on several aspects of this work, and to Dr. P. R. Kennicott for his generous help in programming the General Electric 225 computer. We further gratefully acknowledge the assistance of F. K. Heumann, G. B. Gidley, G. D. Brower, and P. P. Friguletto in preparing and mounting specimens prior to measurement. We also wish to thank J. H. McTaggart for his confirmatory measurements of Seebeck coefficients.

APPENDIX

Tanuma²⁸ and Jain³ have used various semiquantitative arguments to support their conclusions that Bi-Sb alloys become semiconducting in the concentration range from about 5 to 50 at. % Sb. However, one must be careful in ascribing the nature of curves like those shown in Figs. 1-3 as being due to a semiconductor with

a forbidden gap. Such behavior could also be described by various semimetallic models.

Two semimetallic models will be examined. Seebeck coefficient calculations based on these two models will be quantitatively compared with the positive and negative Seebeck coefficients of $+250$ and -260 $\mu\text{V}/^\circ\text{C}$ given by the undoped *p*- and *n*-type samples between 20 and 30°K (samples A and B of Fig. 3 and Table II). Such comparisons support a semiconducting model for $\text{Bi}_{15}\text{Sb}_{15}$ alloys.

Model 1. Consider the semimetallic two-band model shown in Fig. 6. In Fig. 6 the Seebeck coefficient S_T is plotted versus the reduced Fermi energy, $\epsilon = E/kT$, for the case of zero overlap ($E_G = 0$, solid curve) and a large overlap ($E_G = 10kT$, dashed curve), assuming acoustic mode scattering and that the conductivity ratio of the electrons and holes is $\sigma_n/\sigma_p = 60[F_{1/2}(\epsilon)/F_{1/2}(\epsilon_g - \epsilon)]$. The Seebeck coefficient is then given by

$$S_T = \frac{-(\sigma_n/\sigma_p)S_n + S_p}{1 + (\sigma_n/\sigma_p)} \\ = \frac{-(\mu_n/\mu_p)(N_n/N_p)[F_{1/2}(\epsilon)/F_{1/2}(\epsilon_g - \epsilon)]S_n + S_p}{1 + (\sigma_n/\sigma_p)},$$

where S_n , S_p , μ_n , μ_p , N_n , and N_p are the partial Seebeck coefficients,²⁹ mobilities, and density of available states for the electrons and holes, respectively, and $F_{1/2}$ is the Fermi-Dirac integral of order one-half. As is shown in Fig. 6, the magnitude of the negative Seebeck coefficient

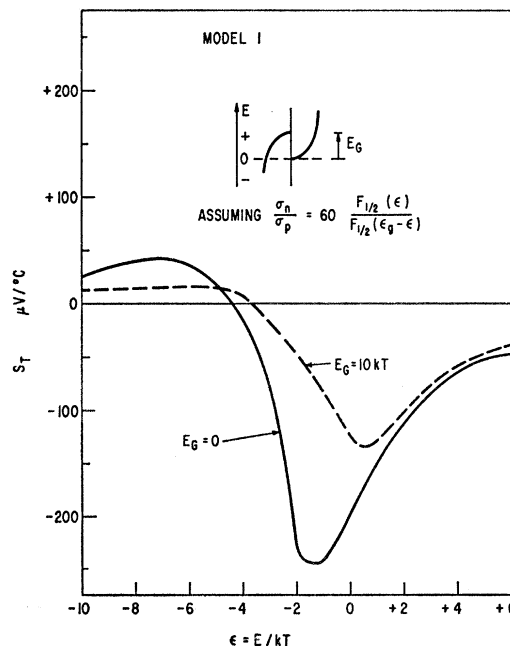


FIG. 6. Two-band semimetallic model with overlap energies, E_G , of 0 and $10kT$, assuming $\mu_n N_n / \mu_p N_p = 60$.

²⁸ S. Tanuma, J. Phys. Soc. Japan 14, 1246 (1959); 16, 2349 (1961); 16, 2354 (1961).

²⁹ See, for example, pp. 342-350 of Ref. 21.

icients at low temperatures given by the undoped *n*-type sample (Fig. 3) could be explained by a suitably doped zero band-gap model, if $(\mu_n/\mu_p)(N_n/N_p) \geq 60$; but such a model *cannot* at the same time account for the large positive Seebeck coefficients given by the undoped *p*-type sample at 20°K.

Model 2. Fig. 7 gives the results of Seebeck coefficient calculations based on the three-band model originally proposed by Jain, Blount, and Cohen³ for Bi-Sb alloys containing about 5% Sb. In this case, the electron and a heavy hole minima are at the same position in energy and a light hole band is spaced below the electron minima at a position near that given by recent magneto-optical measurements of the optical gap in Bi (0.01 to 0.02 eV, see Table I). In this case, the Seebeck coefficient is given by

$$S_T = \frac{-(\sigma_n/\sigma_{HH})S_n + S_{HH} + (\sigma_{LH}/\sigma_{HH})S_{LH}}{1 + (\sigma_n/\sigma_{HH}) + (\sigma_{LH}/\sigma_{HH})},$$

where

$$\sigma_n/\sigma_{HH} = M[F_{1/2}(\epsilon)/F_{1/2}(-\epsilon)],$$

and

$$\sigma_{LH}/\sigma_{HH} = M[F_{1/2}(-\epsilon_0 - \epsilon)/F_{1/2}(-\epsilon)]$$

$$M = \frac{\mu_n N_n}{\mu_{HH} N_{HH}} = \frac{\mu_{LH} N_{LH}}{\mu_{HH} N_{HH}},$$

where $\mu_H, \mu_{H,LH}, N_{HH}, N_{LH}$ are the mobilities and density of states of the heavy- and light-hole bands, respectively, and $\epsilon_0 = E_0/kT$ is the reduced optical gap. The solid curve in Fig. 7 gives the Seebeck coefficient versus ϵ for this model with $M = 100$ and $\epsilon_0 = 6$. Different ϵ_0 's and/or smaller M 's diminish the absolute value of the positive and negative Seebeck coefficients. The dashed curve in Fig. 7 shows the results when $M = 20$ and $\epsilon_0 = 8$. These results indicate that such a model could produce Seebeck coefficients comparable in value to those observed in Fig. 3 if $M \geq 100$. We must now consider what the maximum allowable M is in the Bi-Sb alloy system and/or whether such a model could exist for Bi₃₅Sb₁₅ alloys.

In Bi the largest mobility ratio is for the trigonal components of the electron and hole mobility tensors. At 80 and 300°K, Abeles and Meiboom³⁰ obtained a

³⁰ B. Abeles and S. Meiboom, Phys. Rev. **101**, 544 (1956).

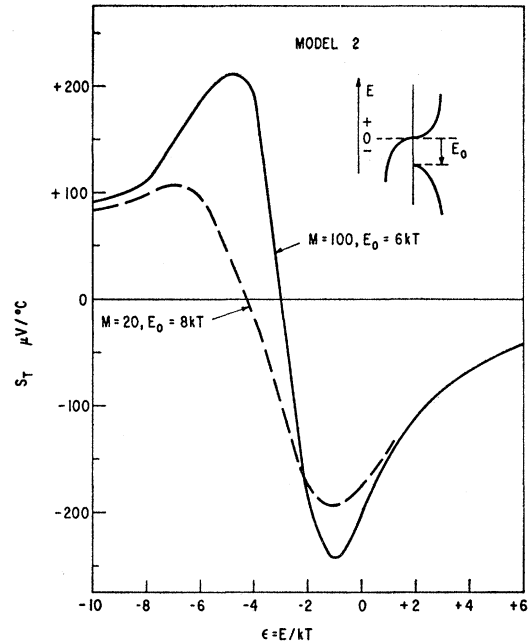


Fig. 7. Three-band semimetallic model with $E_G = 0$, but an optical gap E_0 between the electron and light-hole minima. Solid curve for $M = 100, E_0 = 6 kT$, and dashed curve for $M = 20, E_0 = 8 kT$ where $M = (\mu_n/\mu_{HH})(N_n/N_{HH}) = (\mu_{LH}/\mu_{HH})(N_{LH}/N_{HH})$.

value of about 10, but Zitter¹¹ deduced a value of 30 for this ratio at 4°K. The effective mass ratios at the Fermi surface, as determined by cyclotron resonance experiments, is $m_{HH}/m_n \approx 3$, and the electron-to-heavy-hole valley multiplicity ratio is 3. In Bi, therefore, the ratio $(\mu_n/\mu_{HH})(N_n/N_{HH})$ is at most about 20. Even if one takes into account the factor of two reduction in electron effective mass for electrons at the bottom of the valley,^{7,9} M is at most about 40 since $\mu_n N_n \propto m^{-5/2} m^{3/2}$. It seems unlikely then that in Bi-Sb alloys $M \geq 100$. We must, therefore, conclude that within the limitations of the models examined and the purity of the samples investigated, Bi₃₅Sb₁₅ alloys are real semiconductors. In fact, the original semiconductor model proposed by Jain, Blount, and Cohen³ for Bi-Sb alloys containing between approximately 10 and 30 at. % Sb may be qualitatively correct.